# Structural Changes Accompanying Hydration in Nylon 6

**N. S. Murthy,*† M. Stamm,‡ J. P. Sibilia,† and S. Krimm§**

*Corporate Technology, Allied-Signal Inc., Morristown, New Jersey 07960, Max-Planck-Institut für Polymerforschung, Postfach 3148, Jakob-Welder-Weg 11, D-6500 Mainz, West Germany, and Department of Physics, University of Michigan, Ann Arbor, Michigan 48109.* *Received May 16, 1988; Revised Manuscript Received August 26, 1988*

ABSTRACT: Hydration in polyamides is discussed in terms of three related processes: activation of chains in the amorphous regions, exchange of amide hydrogen, and crystallization. Small-angle neutron-scattering data provide direct evidence for the diffusion of water molecules into the interlamellar amorphous regions of nylon 6. Scattering contrast, resulting from preferential absorption of $D_2O$ by these regions, gives rise to a small-angle peak whose intensity increases with water content. Persistence of ND bands in the infrared spectra of samples in which no neutron-scattering peak could be observed leads us to suggest that disordered chains outside the interlamellar region constitute a major fraction of the amorphous material in the polymer. Swelling of the amorphous matrix reversibly increases the lamellar repeat and decreases the (002) + (202) spacing in the preexisting crystalline lamellae. The change in the (002) + (202) spacing represents lateral rearrangement of the hydrogen-bonded sheets in the crystalline regions, and this is attributed to the changes over the entire fold surface of lamellae due to the specific interactions of water molecules with the noncrystalline segments in the interlamellar regions. Water increases the $\alpha$-crystalline fraction at the expense of both noncrystalline and $\gamma$-crystalline components and above 150 °C hydrolyzes the tie molecules in the interlamellar regions; the tie molecules probably influence the crystalline unit cell parameters. Infrared spectroscopic data indicate that the hydrogen-deuterium exchange in the amorphous regions is reversible, but if this exchange is accompanied by crystallization, then it can be reversed only under conditions more severe than those during crystallization. The changes in the ND doublet (Fermi resonance of ND stretch fundamental with amide II′ and amide III′ bands) at 2420 and 2480 $cm^{-1}$ are analyzed. Hydrogen bonds are stronger in the $\gamma$-crystalline form and the amorphous phase than in the thermodynamically more stable $\alpha$-crystalline form. The 2490 $cm^{-1}$ band in the melt suggests that a significant fraction of the amide groups form hydrogen bonds even in the melt, though these are weaker than in the amorphous and the crystalline phases.

## Introduction

Physical properties of many polymers, especially those that can form hydrogen bonds, are sensitive to moisture. Moisture in nylon 6 and other polymers lowers the glass-transition temperature,[1,2] decreases the Young's modulus,[1] increases water permeability in homopolymers of nylon 6 but decreases it in copolymers of aromatic polyamides, and accelerates the stress-aging characteristics.[3,4] The effect of moisture in nylon 6 films can be readily perceived in the increased pliability of the film. Such changes are usually attributed to the plasticizing effect of water. Several attempts have been made to arrive at a more detailed understanding of the role of water on the physical and mechanical properties of nylon 6.[1,5,6] Even though water penetrates into the amorphous regions of the polymer, there have been suggestions that moisture can affect the ordered crystalline regions as well.[7-9] While calorimetric[1] and dynamic mechanical analysis[10] results suggest specific interactions between the water molecule and the polymer, the evidence is not conclusive.

To better understand the structural features underlying the role of water in polymers, we studied the differential absorption of water by the amorphous and crystalline regions by small-angle neutron scattering (SANS) and small-angle X-ray scattering (SAXS) and used wide-angle X-ray diffraction (WAXD) to study the effect of water on the crystalline regions. Since the hydrogen bond, whose energy is 6–9 kcal/mol in amides,[11] plays an important role in the dynamics of polymer structure, we used infrared (IR) spectroscopy to study the effects of moisture ($D_2O$) on hydrogen bonding in nylon 6, as well as to study the stability of the hydrogen bonds in the crystalline and amorphous regions.

* To whom all correspondence should be addressed.
† Allied-Signal Inc.
‡ Max-Planck-Institut für Polymerforschung.
§ University of Michigan.

## Materials and Methods

Commercial grade Allied nylon 6 films (CAPRAN 77A, thickness ~1 mil, intrinsic viscosity IV = 1.34 dL/g) were used for most of the experiments. Oriented fibers were used to follow small changes in lamellar spacing by SAXS. These yarns (IV = 1.15 dL/g) were spun, conditioned in humid atmosphere, and drawn by ~3:1.

Dry films (~0% moisture) were obtained by keeping the films under dynamic vacuum at 50 °C for 12–24 h. Films of two different moisture content were prepared by suspending the films at 22 °C for at least 16 h over saturated aqueous solutions of $NaHSO_4 \cdot H_2O$ (52% relative humidity; relative humidity will be referred to as humidity in the remainder of the text) and $CaSO_4 \cdot 2H_2O$ (98% humidity). The water content in these films was determined by Karl Fisher titration. $D_2O$ was used for neutron-scattering and infrared measurements. The film at 98% humidity was dried at 50 °C under vacuum for 12–24 h, and SANS and IR measurements were repeated on these dried films. The initial crystalline index in the films was <20% (mixture of $\alpha$ and $\gamma$; in the $\alpha$ form the chains are in the extended-chain conformation and the hydrogen bonds are between antiparallel chains; in the $\gamma$ form the chains are in the $2_1$-helical conformation and the hydrogen bonds are between parallel chains; for details see ref 9 and references therein), and this crystallinity was increased to ~50% by converting some of the amorphous and most of the $\gamma$ fraction into the $\alpha$ form by boiling in water at 100 °C for 2 h.

Films (<1 mil thick) for variable-temperature IR experiments were prepared by heating in the presence of $D_2O$ at 150 °C for about 24 h in a closed steel cylinder. Highly N-deuterated films were obtained in this manner, although some residual NH was left as indicated by the absorptions at 3300 and 1545 $cm^{-1}$. *N*-deuterocaprolactam was obtained by distilling a 0.3 g/mL solution of caprolactam and $D_2O$. This was done twice, using fresh $D_2O$ the second time. Essentially complete N-deuteration of the caprolactam was obtained by this method as evidenced by the lack of NH absorption in the IR spectrum. Polymerization was accomplished by heating the lactam in $N_2$ at 190 °C for 4 h and

0024-9297/89/2222-1261$01.50/0 

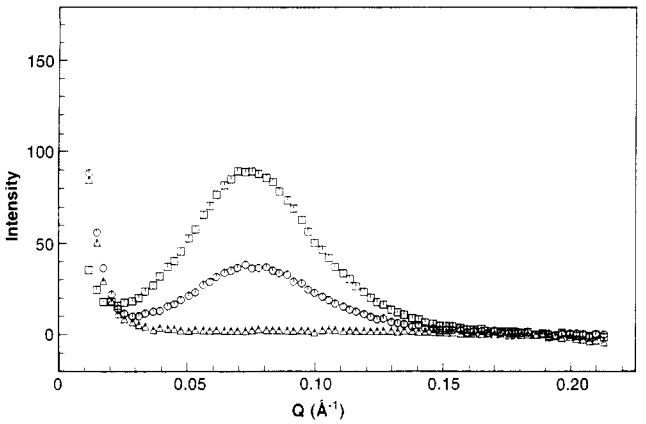


**Figure 1.** Small-angle neutron-scattering (SANS) curves from unannealed nylon 6 films at three concentrations (wt %) of $D_2O$: 0% (△, 0% RH); 5% (○, 52% RH); 11% (□, 98% RH). **Q** on the $x$ axis is the scattering vector $(4\pi \sin \theta)/\lambda$, $\theta$ is half the scattering angle, and $\lambda$ is the wavelength.

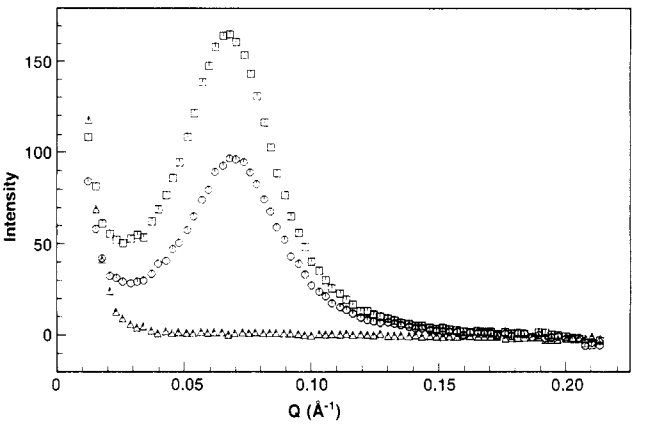


**Figure 2.** SANS curves of annealed nylon 6 films at three concentrations (wt %) of $D_2O$: 0% (△, 0% RH); 4% (○, 52% RH); 8% (□, 98% RH).

then for 20 h at 260 °C. The polymer was then ground and extracted with $D_2O$ to remove residual monomer. Infrared spectra of films molded from this material were essentially the same as those obtained from $D_2O$-treated nylon 6, and only the data from $D_2O$-treated nylon 6 will be presented.

WAXD photographs were obtained on a Unicam Camera with a sample-to-film distance of 4 cm using Ni-filtered Cu radiation. Quantitative wide-angle data were obtained on a Philips diffractometer in parafocus geometry with graphite-monochromatized Cu radiation. WAXD data were analyzed to determine the fractions of the $\alpha$- and the $\gamma$-crystalline forms, as well as the total crystallinity. The diffractometer scan between 15° and 30° $2\theta$ was resolved into two $\alpha$- and two $\gamma$-crystalline peaks (see ref 9 and references therein) and an amorphous halo. An X-ray crystalline index and the fractions of the $\alpha$ and $\gamma$ components were obtained from the ratio of the area under the corresponding crystalline peaks to the area under the scattering curve. These values are reported here as percent crystallinity, percent $\alpha$, and percent $\gamma$. Since only the $\alpha$-crystalline peaks can be easily and reliably resolved, the positions of these peaks, corresponding to (200) and (002) + (202) reflections, were measured.

SAXS data were obtained using Ni-filtered Cu radiation with a position sensitive proportional counter on a Franks camera.[12] SANS data were obtained on a two-dimensional detector at Brookhaven National Laboratories. The samples were kept sealed in quartz containers. Monochromatization was achieved by a multilayer plate. The sample-to-detector distance was 190 cm, and the wavelength was 5.11 Å. Scattered intensities were averaged around azimuth to eliminate the effect of slight orientation present along the rolling direction. These averaged intensities were then put on the same scale by dividing by the monitor counts, sample thickness, and sample absorption. The intensities were also corrected for counting efficiency by using the Lupolen sample as a uniform scatterer. The intensity at $Q = 0.19$ Å$^{-1}$ ($Q = (4\pi \sin \theta)/\lambda$) was assumed to be completely background scattering and was subtracted from each of the scattering curves. The low-angle spacing, or the lamellar spacing, was calculated by applying Bragg's law to the position of the small-angle peak. Coherence length was evaluted from the Scherrer equation and the width of the small-angle peak.

IR spectra on nylon 6 films exposed to $D_2O$ were obtained at room temperature on a Perkin-Elmer 983 spectrometer with a resolution of 3 cm$^{-1}$ at 1000 cm$^{-1}$. Spectra from nylon 6 films as a function of temperature on N-deuterated polymers and iodinated film were obtained on a Beckman IR 12 spectrometer. Viscosity of nylon 6 was measured with a 0.52% polymer solution in $m$-cresol at 25 °C in a capillary viscometer.

## Results

**Small-Angle Scattering.** SANS data from unannealed and annealed films at 0%, 52%, and 98% humidity ($D_2O$) are given in Figures 1 and 2. The data are summarized in Table I. The high background level is due to the incoherent scattering of hydrogen. Without the swelling of nylon 6 with $D_2O$, there is essentially no coherent scattering contribution; the negative coherent scattering length of hydrogen largely cancels out the positive scattering lengths of carbon, nitrogen, and oxygen, thus reducing the mean scattering density of a nylon 6 monomer to zero. Therefore, the long-spacing arising from the differences in the density of amorphous and crystalline regions is hardly detected in neutron-scattering experiments. In films swollen with $D_2O$, the observed neutron scattering is due to the nonuniform distribution of $D_2O$ over distances of hundreds of angstroms in some regions of the film. The small-angle peak at a Bragg spacing of ca. 90 Å is due to a separation between $D_2O$-rich and $D_2O$-poor regions. It is evident from the SANS data that the observed peak is correlated with $D_2O$ absorption: the intensity increases with $D_2O$ content (Figures 1 and 2). This SANS peak is weak (<7% of the value in films at 98% RH) in both crystalline and amorphous films after removal of $D_2O$ by pumping under vacuum. Thus, the major contribution to the neutron-scattering contrast is from $D_2O$ and not from exchanged deuterium on the amide nitrogen.

**Table I**
**Results of Analysis of SANS Data**

| sample | RH, % | wt % $D_2O$ | low-angle spacing, Å | coherence length, Å |
|---|---|---|---|---|
| unannealed | 52 | 4.8 | 84 | 220 |
| | 98 | 11.1 | 84 | 220 |
| annealed | 52 | 4.2 | 91 | 310 |
| | 98 | 7.5 | 91 | 310 |

SAXS and SANS experiments with oriented films and fibers confirm that the observed peak is indeed associated with the interlamellar spacing. As in many polymers with folded chain lamellae, the low-angle spacing and the coherence length are smaller in unannealed films than in annealed films (Table I). Additionally, the integrated intensity in unannealed films is about half of that in annealed films (Figures 1 and 2), although the unannealed films take up about twice as much moisture. It is likely $D_2O$ is present in regions which do not contribute to the neutron-scattering contrast. We also noticed that background, which is mostly incoherent scattering of hydrogen, is smaller in $D_2O$-rich films than in films not exposed to $D_2O$. We do not fully understand this observation and believe that this is partially due to the dilution effect of $D_2O$.

The lamellar spacings from SAXS measurements on samples used for SANS experiments were the same as those listed in Table I. X-rays are mostly sensitive to

Table II
Results of Analysis of Wide-Angle Data

| unannealed | | | | annealed | | | | |
|---|---|---|---|---|---|---|---|---|
| wt % $H_2O$ | crystalline index, % | $\alpha$, % | $\gamma$, % | wt % $H_2O$ | crystalline index, % | $\alpha$, % | $\gamma$, % | $\Delta d$, Å |
| 0 | 25 | 19 | 6 | 0 | 39 | 34 | 5 | 0.650 |
| 4.8 | 27 | 21 | 6 | 4.2 | 38 | 33 | 5 | 0.659 |
| 11.1 | 32 | 27 | 5 | 7.5 | 39 | 35 | 4 | 0.673 |

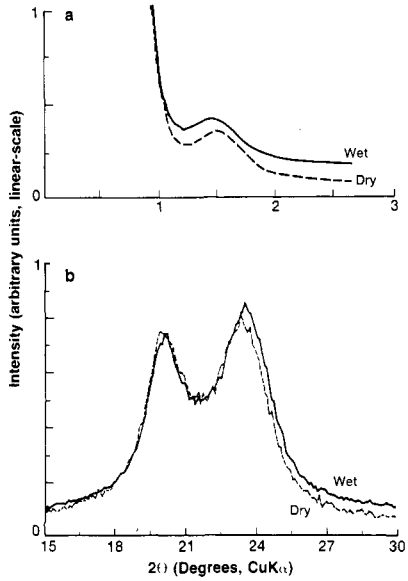


**Figure 3.** Small-angle (a) and wide-angle (b) X-ray diffraction scans of nylon 6 fibers at 0% and 98% humidity. SAXS scans are along the fiber axis. WAXD scans were obtained in parafocus geometry and are therefore equivalent to an equatorial scan. The curves in this and the next figure have been vertically off-set.

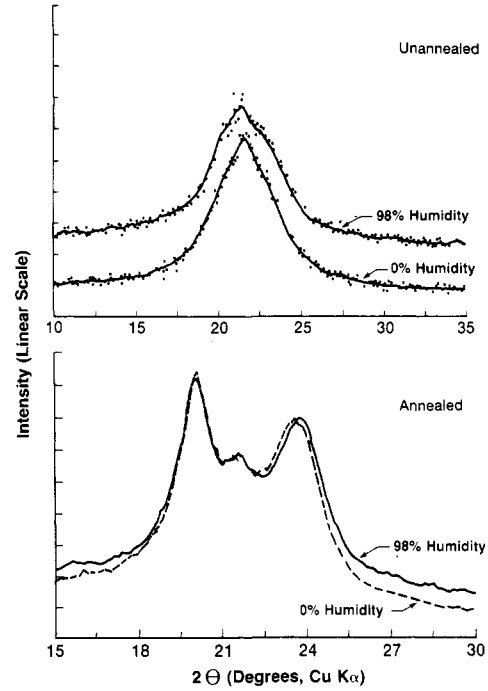


**Figure 4.** Wide-angle X-ray diffraction curves (parafocus geometry) of unannealed and annealed nylon 6 films at 0% and 98% humidity.

carbon, nitrogen, and oxygen, and the scattering from hydrogen is negligible. The mean structure factor of a nylon 6 monomer is significantly different from zero. Therefore, with X-rays, the density difference between amorphous and crystalline regions gives rise to the well-known long-period reflection. Figure 3a shows SAXS data from an oriented fiber (crystallinity ~50%) after exposure to 0% (vacuum dried) and 98% ($CaSO_4 \cdot 2H_2O$) humidity. SAXS data from several such fibers show that the lamellar spacing expands by 1.6 Å, from 78.2 to 79.8 Å, in going from 0% to 98% humidity. The difference is small, slightly more than $1\sigma$ ($\sigma$ = 1.3 Å), but was consistently observed in all of the six dry and the six wet samples. This result is consistent with an earlier published result.[13] Further, we observed that this change in the lamellar spacing is reversible.

**Wide-Angle X-ray Diffraction.** Wide-angle X-ray diffraction scans of annealed nylon 6 films at two levels of moisture content (0% and 98% humidity) are shown in Figures 3 and 4. The results derived from Figure 4 are summarized in Table II and show that amorphous nylon 6 films readily transform into an $\alpha$-rich film upon annealing in water at 100 °C for 2 h. Also, note that even at room temperature, moisture brings about a slight increase in the crystallinity and promotes the growth of the $\alpha$ fraction at the expense of some of the disordered phase. These findings are consistent with our earlier result obtained from nylon 6 fibers.[9]

Although moisture has very little effect on the total crystallinity of the annealed fibers, it does reversibly shift the positions of the crystalline Bragg peak (Figures 3b and 4b). This can be accurately expressed in terms of $\Delta d$, the difference in the $d$ spacings of the (200) and (002) + (202) peaks. It has been shown that $\Delta d$ values are more reliable than peak positions themselves and that an increase in $\Delta d$ correlates with an increase in the crystalline density and crystallite size, and therefore with crystalline perfection.[14] This $\Delta d$ parameter is useful in following small changes in unit-cell parameters, whereas the actual $d$ spacings corresponding to individual peaks are sensitive to sample position and the alignment of the diffractometer. The (200) peak, to a first approximation, represents the distance between hydrogen-bonded chains and does not change significantly. Therefore, one could attribute the changes in $\Delta d$ to the changes in the positions of the second intense crystalline peak, (002) + (202), which in general terms corresponds to the distance between hydrogen-bonded sheets, but more specifically reflects the shape or the geometry of the unit cell. For the sample shown in Figure 3b, $\Delta d$ increases from 0.600 to 0.625 Å upon exposure to 98% humidity and decreases back to 0.600 Å when the humidity is reduced to 0%. For the sample in Figure 4b, $\Delta d$ increases from 0.65 to 0.67. SAXS and WAXD data on the same sample in Figure 3 show that changes in the $c$ and the $\beta$ parameters of the unit cell are accompanied by changes in the lamellar spacings.

**Infrared Spectroscopy.** To investigate the role of water in bringing about structural changes, we carried out infrared spectroscopic measurements on several nylon 6 films exposed to $D_2O$ and on N-deuterated nylon 6 films. Infrared spectra of an unannealed film (less than 20% crystallinity) before and after exposure to $D_2O$ at 98% humidity (11 wt.% $D_2O$ uptake; spectrum obtained in a stream of dry nitrogen) are shown in parts a and b of Figure 5, respectively. Also shown in this figure are the spectra from the same film after drying under vacuum at 50 °C (curve c) and after exchanging with $H_2O$ at 70 °C (curve d). In this paper we concentrate on the ND bands

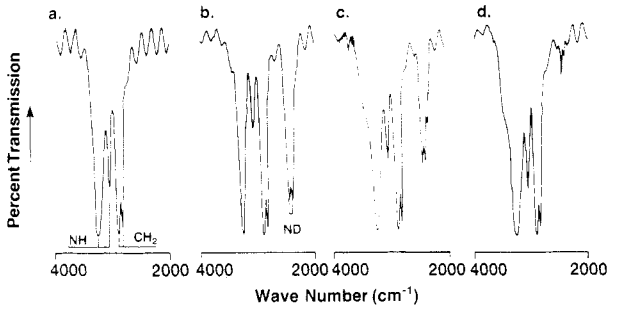


**Figure 5.** Infrared spectra of unannealed nylon 6 films. (a) Dried at 40 °C under vacuum for 12 h. (b) Film in curve a after exposure to 98% relative humidity (11% $D_2O$). (c) Film in curve b after drying at 50 °C under vacuum. (d) Film in curve c after exchanging with $H_2O$ at 70 °C.

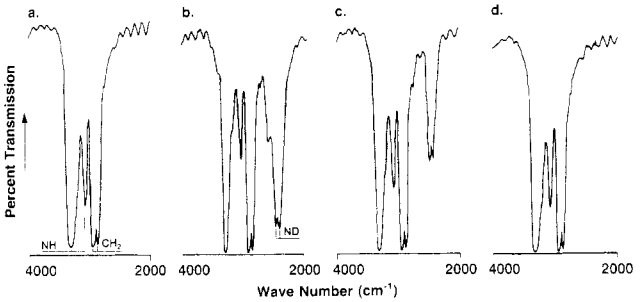


**Figure 6.** IR spectra of annealed film (a), after exposure to 98% humidity $D_2O$ (b), after drying at 50 °C under vacuum (c), and after exposure to water at 70 °C (d).

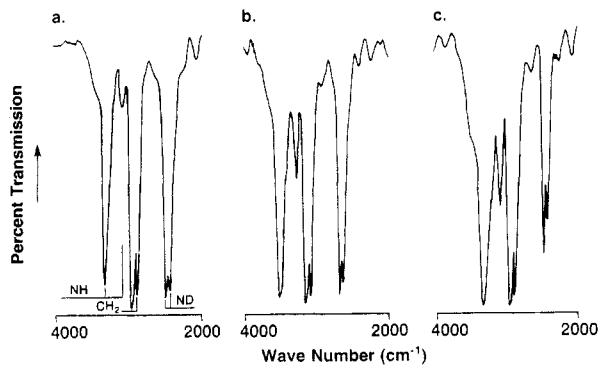


**Figure 7.** Infrared spectra of nylon 6 films treated with $D_2O$ at 100 °C (a), after drying at 50 °C under vacuum (b), and after exchange with $H_2O$ at 70 °C (c).

at 2470–2480 $cm^{-1}$ and at 2420 $cm^{-1}$. For the sake of convenience, we will label the higher and the lower frequency bands as the 2480 and 2420 $cm^{-1}$ bands, respectively.

In a second experiment, highly crystalline nylon 6 film was prepared by annealing in water at 100 °C. The film was dried under vacuum at 50 °C for 10 h, and then exposed to 98% humidity ($D_2O$ uptake 7.5 wt %). The film was then dried under vacuum at 50 °C for 16 h. Infrared spectra of this starting film, the $D_2O$ exposed film (in a stream of dry nitrogen), and the vacuum-dried film are shown in parts a, b, and c of Figure 6, respectively. As before, a fourth spectrum (Figure 6d) was obtained after exchanging with $H_2O$ at 70 °C. The IR spectra obtained from amorphous and crystalline films exposed to $D_2O$ and sealed between quartz plates were similar to those shown in Figures 5b and 6b, respectively.

In a third experiment, the unannealed films were exposed to $D_2O$ at 100 and 140 °C to achieve maximum possible N-deuteration. The spectra of the deuterated films are shown in Figures 7a and 8a. The spectra of these films when dried under vacuum at 50 °C (Figures 7b and

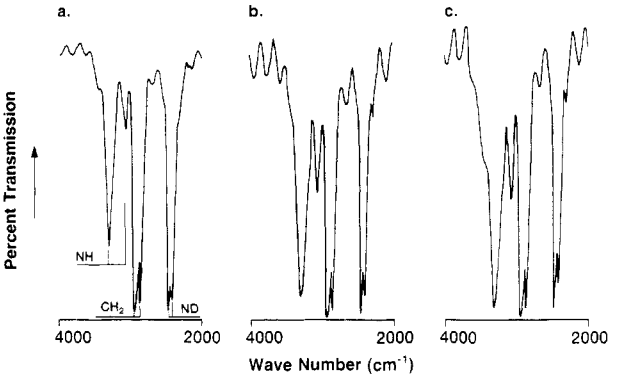


**Figure 8.** Infrared spectra of nylon 6 film treated with $D_2O$ at 140 °C (a), after drying at 50 °C under vacuum (b), and after exchange with $H_2O$ at 70 °C (c).

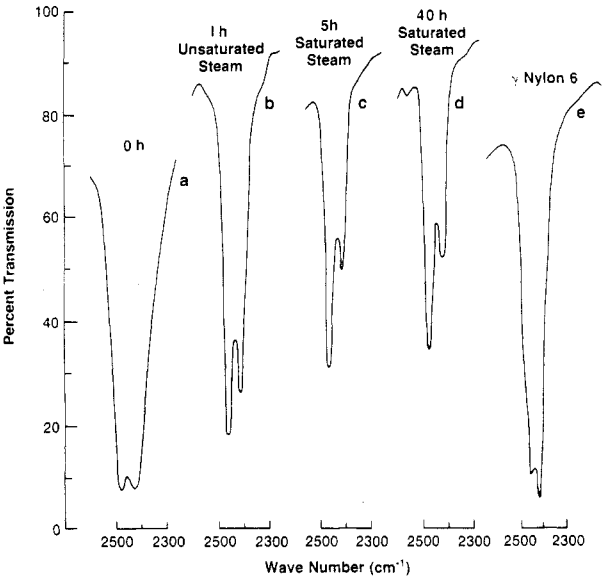


**Figure 9.** Variations in the shape and the relative intensities of the 2420 and 2480 $cm^{-1}$ ND absorption bands upon exposure to steam ($H_2O$). For comparison, the spectrum from the $\gamma$ form of nylon 6 is also shown.

8b) and after exchanging with $H_2O$ at 70 °C (Figures 7c and 8c) were also obtained. Note the increase in the ratio of the intensity of the two ND stretch bands, $A(2480)/A(2420)$, in these samples in going from a to b and c, as well the decrease in half-widths of these bands, relative to those in Figures 5 and 6 (except Figure 5d).

Figures 5–7 show that, as the $D_2O$-exposed films are dried under vacuum at 50 °C and then further exposed to $H_2O$ at 70 °C, the intensity of both of the ND bands decreases and the ratio of the intensities of the 2480 $cm^{-1}$ and 2420 $cm^{-1}$ bands increases. This is also shown in Figure 9 in which IR spectra of a quenched and then deuterated nylon 6 film exposed to steam ($H_2O$) for various lengths of time are given. In the first hour of exposure, $A(2480)/A(2420)$ increases from 0.996 to 1.31. After about 5 h, the ratio increases further to 1.72. The intensity of the two bands decreases only slightly but the ratio remains unchanged upon further (up to 40 h) exposure to steam. For comparison, the spectrum of a deuterated $\gamma$-nylon 6 film (obtained by $KI_3$ treatment) is also given, showing the reversal in the intensities of these two bands.

In connection with a further analysis of this doublet, we have examined the effect of temperature on the spectrum. This is shown in Figure 10, for an essentially amorphous (15–20% crystallinity, mixture of disordered $\alpha$ and $\gamma$ forms) film. These IR spectra, obtained and presented in absorbance mode unlike the percent transmission in Fig-

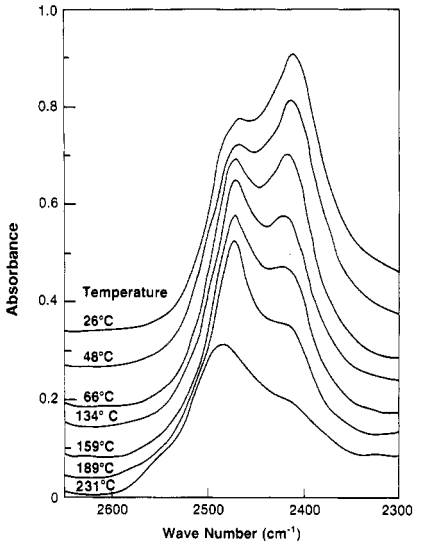


**Figure 10.** ND bands in N-deuterated nylon 6 as a function of temperature. These spectra, unlike in Figures 5–9, were recorded in absorbance mode.

ures 5–9, being on logarithmic scale show small differences at various temperatures. On heating, the 2468 $cm^{-1}$ band shifts to 2473 $cm^{-1}$ between 48 and 66 °C near the glass-transition temperature of nylon 6 (and finally to over 2490 $cm^{-1}$ in the melt at 260 °C), and its intensity relative to the ~2420 $cm^{-1}$ band reverses above 66 °C. A shoulder at 2550 $cm^{-1}$ provides evidence for some unassociated ND bonds. Upon quenching, the hydrogen bonds, rather than retaining their conformation in the melt, rapidly rearrange themselves to give the 2418 and 2468 $cm^{-1}$ bands.

## Discussion

**Water Absorption in Nylon 6.** The SANS lamellar peak arises from periodic modulations imposed on the distribution of $D_2O$ by amorphous and crystalline regions in the polymer. The amount of water absorbed decreases with an increase in crystallinity, from 11% for the least crystalline film to 8% for the most crystalline film. This suggests that moisture is preferentially absorbed into the amorphous regions. Let us assume that each amide group coordinates with one water molecule. Then the maximum amount of water that nylon 6 can absorb is 13.5 wt %. The calculated water contents in the least crystalline (~20% crystallinity, mixture of disordered $\alpha$ and $\gamma$ forms) and the most crystalline (~50% crystallinity) samples are, respectively, 11% and 7%. These are in agreement with the observed values (11% and 7.5%), suggesting that on average one water molecule is closely associated with a CONH group in the nylon 6 chains in the amorphous regions.

We now examine three processes which are likely to accompany diffusion of $D_2O$ or $H_2O$ into nylon 6: (1) Upon exposure to humidity, $D_2O$ diffuses into the amorphous regions, acts as a plasticizer, and decreases $T_g$.[1,2,6] This is probably due to the disruption of the hydrogen bonds between nylon 6 chains in favor of hydrogen bonds between the amide groups and the water molecules (perhaps with a water molecule acting as a bridge between two CONH groups). This water, which can be easily desorbed, increases the mobility of the amorphous regions (activation) and accounts for the 5% and 11% $H_2O$ (or $D_2O$) at respectively 52% and 98% humidity in unannealed films, and 4% and 8% $H_2O$ (or $D_2O$) at respectively 52% and 98% humidity in annealed films. (2) During the exposure to $D_2O$, NH to ND exchange occurs. This exchange is reversible in the amorphous regions. (3) This NH–ND exchange, and therefore absorption of water, may be accompanied by the crystallization of nylon 6. The extent of reversibility of NH–ND exchange in crystalline regions depends on the severity of the conditions under which the initial exchange and crystallization takes place.

**Effect of Water on Crystalline Regions.** Diffusion of water into nylon 6 has a slight but noticeable effect on the position of the Bragg peaks from the crystalline fraction (Figures 3 and 4); the dimensional change, as seen in the position of the (002) + (202) reflection (which is most marked), is ~0.025 Å. This represents a reorganization of the hydrogen-bonded sheets relative to each other, and these changes are too small to be caused by the diffusion of water into the crystalline lattice. Moisture diffuses primarily into the amorphous regions.

How does the moisture change the lateral organization of the hydrogen-bonded sheets in the crystalline lamellae, even in the annealed samples (Table II), without entering the lattice? In contrast to an earlier proposal,[7] we suggest that this is not due to the direct diffusion of $H_2O$ into the crystal lattice but is caused by the swelling of the noncrystalline regions. Specific interactions of water with the noncrystalline segments in the interlamellar regions (fold and tie molecules) could uniformly affect the entire fold surface of the lamellae and thus cause the hydrogen-bonded sheets to shift relative to each other in the equatorial plane within the crystalline lamellae. These changes are measured as changes in the $c$-axis dimension or the $\beta$ angle of the unit cell. While humidity increases the lamellar spacing and decreases the (002) + (202) spacing, upon redrying the sample to 0% humidity, a decrease in lamellar spacing is accompanied by an increase in the (002) + (202) spacing. Thus, the effect of moisture (i.e., swelling) on the lamellar spacing and on the packing of the chains within the crystalline lamellae is reversible. More importantly, the changes within the lamellae reflect the changes in the interlamellar region. We came to similar conclusions based on the analysis of data from annealed fibers.[14]

**Water and Chain Scission.** At or above 155 °C, water preferentially hydrolyzes chains in the amorphous domains, while at the same time increasing the crystalline density. The solution viscosity of an amorphous film decreases from 1.33 to 0.25 dL/g; the crystallinity as measured by XRD approaches 70–75%, and $\Delta d$, the separation of the two $\alpha$-peaks (200) and (020) + (220), is 0.72–0.75 Å. The crystallinity is 15–20% higher than that obtained for nylon 6 of viscosity 1.33 dL/g; $\Delta d$ for a highly crystalline fiber is usually ~0.73. The high crystallinity and $\Delta d$ must be due to the dissolution of the chains in amorphous regions, probably by the scission of the tie molecules. It is likely that before dissolution the polymer swells, the interlamellar spacing increases, and strains are placed on the tie molecules. These tie molecules, which undergo hydrolysis, affect the packing of the chains in the crystalline lamellae as discussed earlier. When a film with an initial crystallinity of 15–20% was partially hydrolyzed with water at 155 °C, the viscosity decreased from 1.33 to 0.76 dL/g, and the crystallinity increased to ~60% with $\Delta d$ of ~0.72. Thus, water at higher temperatures (>155 °C) causes significant chain scission, and this is greater in a film with a higher amorphous fraction. These results suggest that hydrolysis and diffusion of water occurs only in the amorphous regions.

**Effect of Water on Amide Groups (Infrared Results).** Before discussing the results of H → D exchange, it should be noted that the relative intensities of the two bands near 2480 and 2420 $cm^{-1}$ are a function of at least

two factors. First, these bands arise from Fermi resonance between the ND stretch fundamental and a combination between amide II′ (CC and CN stretch, 1470 $cm^{-1}$) and amide III′ (ND in-plane bend, 970 $cm^{-1}$)[15-17] and are therefore very sensitive to small changes in hydrogen bond geometry and strength. This is illustrated in Figure 10: increases in temperature weaken the hydrogen bond, raising the ND stretch frequency and lowering the amide III′ frequency, and thus result in a change from a combination that is higher in frequency than the fundamental (and therefore $A(2480)/A(2420) < 1$, similar to the case of β-poly(L-alanine)[17]) to one in which the opposite is true. Second, aside from local conformational effects, the fundamental ND stretch frequency is expected to be different for α- and γ-nylon 6. This is a result of the different hydrogen bond geometries in the two structures. For α-nylon 6, the N···O distance is 2.806 Å and the C=O bond length is 1.218 Å,[18] whereas for γ-nylon 6 the corresponding values are 2.801 Å and 1.23 Å.[19] These distances, as well as the frequency of the amide V band (NH out-of-plane bend) at 692 $cm^{-1}$ for the α form and 711 $cm^{-1}$ for the γ form,[20] indicate that the hydrogen bonds in γ-nylon 6 are stronger and therefore that its ND stretch frequency is lower. The higher ND stretch and lower amide II′[20] frequencies of α-nylon 6 result in a combination that is at lower frequency than the fundamental, and therefore to $A(2480)/A(2420) > 1$. In the γ form, lower ND stretch and higher amide II′ frequencies result in a combination that is at a higher frequency than the fundamental, and therefore to $A(2480)/A(2420) < 1$. Thus, the observed value of $A(2480)/A(2420)$ is a result of the superimposed contributions from α- and γ-nylon 6, as well as a contribution from the amorphous component.

Data in Figures 5–9 illustrate the variations in the 2480 and 2420 $cm^{-1}$ Fermi resonance bands in the three forms (amorphous, α crystalline, and γ crystalline) of nylon 6. The ratio $A(2480)/A(2420) \approx 1$ in all instances in which ND bonds are not likely to be present in the α- or the γ-crystalline forms; e.g., the quick-quenched samples exposed to $D_2O$ (Figures 5b and 9a), and the highly crystalline films exposed to $D_2O$ (Figures 6b,c). The ratio $A(2480)/A(2420)$ increases as the number of ND bonds in the amorphous region is decreased either by partial crystallization of the N-deuterated chains into the α form (Figure 5c) or by reexchange with $H_2O$ (Figure 9b,c). $A(2480)/A(2420) \gg 1$ when N-deuterated chains are incorporated in the α-crystalline form by crystallizing nylon 6 in $D_2O$ at elevated temperatures (100 °C, in Figure 7 and 140 °C in Figure 8). The ratio $A(2480)/A(2420)$ further increases and the peaks become narrower as the ND bonds are selectively depleted in the amorphous phase by drying (Figures 7b and 8b) and reexchange with $H_2O$ (Figures 5d, 7c, 8c, and 9d). Finally, in the γ-crystalline form (Figure 9e), obtained by $I_2$/KI treatment followed by removal of iodine by sodium thiosulfate, the peaks are sharp and $A(2480)/A(2420) < 1$. The frequencies of these two absorption bands, not just the intensity ratios, depend on the sample history. While the 2420 $cm^{-1}$ band does not shift significantly, the 2480 $cm^{-1}$ band is observed at ca. 2490, 2470, 2475, and 2480 $cm^{-1}$ in, respectively, molten, amorphous, α-crystalline, and γ-crystalline forms of nylon 6. (The corresponding NH bands are at 3298 and 3065 $cm^{-1}$ for the α form, and at 3297 and 3096 $cm^{-1}$ for the γ form.[20]) The interpretation of these changes will depend on a detailed analysis of fundamental frequencies. However, the changes in the ratio $A(2480)/A(2420)$ discussed above strongly suggest that the hydrogen bonds are weaker in molten nylon 6 and in the α-crystalline form than in the amorphous and the γ-crystalline forms.

It is clear from Figures 5 and 6 that deuteration of NH groups in these amide samples occurs at room temperature, that it is far from complete, and that it is reversible under certain circumstances. The first point is clear from the presence of an ND stretch band after vacuum drying, Figures 5c and 6c (the slightly stronger bands before drying, Figures 5b and 6b, undoubtedly reflect the presence of $D_2O$ in the sample); the second point is evident from the continued presence of a strong NH stretch band (Figures 5c and 6c); and the last point can be seen from the decreased ND intensity after treatment with $H_2O$ at 70 °C (Figures 5d and 6d). Under the latter circumstances, some ND absorption still remains for the unannealed sample (Figure 5d) but is absent for the annealed sample (Figure 6d). We believe that this can be understood in terms of the partial crystallization of the amorphous film during $D_2O$ treatment. These crystallized regions would have incorporated ND groups into the lamellae and would thus be unable to reexchange. On the other hand, in annealed films, $D_2O$ or $H_2O$ diffuses primarily into the amorphous regions and is thus not accompanied by crystallization. The exchange is thus essentially complete. This is strongly supported by the results on the initially highly crystalline and highly deuterated films, Figures 7 and 8. Although some NH is still present, the ND band is much more intense, reexchange by $H_2O$ at 70 °C is very much less (Figures 7c and 8c), and the reexchange is significantly less for the film deuterated at 100 °C (Figure 7) as compared to the film deuterated at 140 °C (Figure 8). All of these results are consistent with having amorphous regions that are significantly accessible, and crystalline regions that are essentially inaccessible, to water.[21-23]

**Absorption of Water by the Amorphous Phase.** Given the above conclusion, it is still necessary to explain why dried films show no, or only a weak, SANS peak even though the IR spectrum gives evidence of the presence of a large number of ND groups (Figures 5c and 6c). Upon drying the film under vacuum, the SANS peak intensity is less than 7% of the wet film (98% RH) in both the amorphous (unannealed) and the crystalline (annealed) films, while the ND band intensity is ~75% of the wet (98% RH) film. It might be possible to explain this observation in unannealed film by assuming uniform distribution of the deuterated chains throughout the sample as the N-deuterated chains crystallize during exposure to $D_2O$. This would eliminate the neutron-scattering contrast while ND bands could still be present in the IR spectrum. We believe that this explanation is incomplete, especially in annealed films in which no ND groups are incorporated into the crystalline lamellae. We suggest that a major contributor to this effect is the presence of two kinds of amorphous regions: those separating regularly spaced lamellae and those not in this category. If the former comprise a relatively small percentage of the total amorphous component, then removal of the $D_2O$ (which provides the major neutron-scattering contrast) from these regions could reduce the SANS peak to a small value (the number of remaining ND groups being insufficient to provide an observable contrast). The amorphous component not between lamellae of course cannot give rise to a SANS peak, since the $D_2O$ is relatively uniformly distributed, but it will retain a significant ND contribution after the $D_2O$ is removed.

These conclusions are in surprising agreement with our SANS data from unannealed and annealed films. Although unannealed films take up twice as much $D_2O$ as

the annealed films, the SANS peak intensity in unannealed film is about half that in the annealed film. This could only mean that a small fraction of absorbed $D_2O$ in unannealed film diffuses into the interlamellar region, while a large fraction of absorbed $D_2O$ diffuses into the amorphous regions outside the lamellar stacks; only the first fraction contributes to neutron-scattering contrast and SANS intensity. Our conclusions are also consistent with the lamellar spacing obtained from SAXS and the crystallite size derived from WAXD. In one fiber sample in which 53% of the polymer was amorphous, the lamellar spacing was 71 Å and the lamellar thickness (crystallite size along the fiber axis, corrected for instrumental and microstrain broadening) was 62 Å.[9] Thus, the fraction of the amorphous polymer in the interlamellar region is 13%, about one-fourth of the total amorphous material.

## Conclusion

We have shown that water molecules diffuse almost exclusively into the amorphous regions of nylon 6. Diffusion of water into the interlamellar regions swells this amorphous matrix, increases the lamellar repeat, decreases the unit cell volume in preexisting lamellae, and at elevated temperatures hydrolyzes the tie molecules. Diffusion of water into the amorphous region outside the lamellar stacks, which can be a significant fraction, lowers the glass-transition temperature, decreases the modulus, and crystallizes the polymer.

**Acknowledgment.** The help of Dr. D. Schneider (Brookhaven National Laboratories) during the neutron-scattering experiments is greatly acknowledged. We thank Drs. A. J. Signorelli and I. Palley for discussions on the interaction between amorphous and crystalline regions, K. O'Brien for providing some of the IR spectra, and C. Lombardo for viscosity measurements. This work was partially supported by DOE.

**Registry No.** Nylon 6, 25038-54-4; water, 7732-18-5.

## References and Notes

(1) Reimschuessel, H. K. *J. Polym. Sci., Polym. Chem. Ed.* **1978**, *16*, 1229.
(2) Yokouchi, M. *J. Polym. Sci., Polym. Phys. Ed.* **1984**, *22*, 1635.
(3) Bubeck, R. A.; Kramer, E. J. *J. Appl. Phys.* **1971**, *42*, 4631.
(4) Verma, A.; Deopura, B. L.; Sengupta, A. K. *Text. Res. J.* **1984**, *54*, 92.
(5) Deopura, B. L. Sengupta, A. K.; Verma, A. *Polym. Commun.* **1983**, *24*, 287.
(6) Jin, X.; Ellis, T. S.; Karasz, F. E. *J. Polym. Sci., Polym. Phys. Ed.* **1984**, *22*, 1701.
(7) Campbell, G. A. *J. Polym. Sci., Polym. Lett.* **1969**, *7*, 629.
(8) Heuvel, H. M.; Huisman, R. *J. Appl. Polym. Sci.* **1981**, *26*, 713.
(9) Murthy, N. S.; Aharoni, S. M.; Szollosi, A. B. *J. Polym. Sci., Polym. Phys. Ed.* **1985**, *23*, 2549.
(10) Birkinshaw, C.; Buggy, M.; Daly, S. *Polym. Commun.* **1987**, *28*, 286.
(11) Jorgensen, W. L.; Swenson, C. J. *J. Am. Chem. Soc.* **1985**, *107*, 1489.
(12) Murthy, N. S. *Norelco Rep.* **1984**, *30*, 35.
(13) Hinrichsen, G. *Colloid Polym. Sci.* **1978**, *256*, 9.
(14) Murthy, N. S.; Minor, H.; Latif, R. A. *Macromol. Sci. Phys.* **1987**, *26*, 427.
(15) Cannon, C. G. *Spectrochim. Acta* **1960**, *16*, 302.
(16) Garton, A.; Phibbs, M. K. *Makromol. Chem., Rapid Commun.* **1982**, *3*, 569.
(17) Krimm, S.; Dwivedi, A. M. *J. Raman Spectrosc.* **1982**, *12*, 133.
(18) Holmes, D. R.; Bunn, C. W.; Smith, D. J. *J. Polym. Sci.* **1955**, *17*, 159.
(19) Bradbury, E. M.; Brown, L.; Elliott, A.; Parry, D. A. D. *Polymer* **1965**, *6*, 465.
(20) Schmidt, P.; Schneider, B. *Collect. Czech. Chem. Commun.* **1963**, *28*, 2556.
(21) Koshimo, A. *J. Appl. Polym. Sci.* **1965**, *9*, 55.
(22) Koshimo, A.; Tagawa, T. *J. Appl. Polym. Sci.* **1965**, *9*, 117.
(23) Schmidt, P.; Schneider, B. *Collect. Czech. Chem. Commun.* **1966**, *31*, 1896.

# Structural and Energetic Analyses of the $\alpha$ to $\beta$ Phase Transition in Poly(butylene terephthalate)

**Robert P. Grasso, Brian C. Perry, Jack L. Koenig, and Jerome B. Lando***

*Department of Macromolecular Science, Case Western Reserve University, Cleveland, Ohio 44106.* *Received June 2, 1988; Revised Manuscript Received August 22, 1988*

ABSTRACT: The crystal structure of the stressed $\beta$ phase of PBT was refined by using intensity data from recently obtained high-quality X-ray fiber diffraction patterns. The crystallographic *c* axis was found to be tilted 1.5° away from the macroscopic fiber axis. This was manifested in determinable displacements of the reflections above and below their respective layer lines. These displacements were beneficial since they allowed several overlapping reflections to be resolved and they confirmed several indexing solutions. The reported structure is preferred over those reported earlier on the basis of better agreement with observed intensity data, Hamiltonian statistics of parameters refined, and potential energy calculations. The energy calculations also indicate that the $\alpha$ form, with its $A^+TA^-$ tetramethylene conformation, is favored over the $\beta$ phase (ttt conformation) predominantly due to intermolecular packing contributions.

## 1. Introduction

Poly(butylene terephthalate), PBT, is a member of the series of aliphatic terephthalate polyesters which includes such commercially successful materials as poly(ethylene terephthalate), PET. A great deal of interest in PBT has been generated recently because fibers of the polymer exhibit a reversible crystal–crystal phase transition when uniaxially drawn. This transition was first discovered by Boye and Overton in 1974.[1] The relaxed or $\alpha$ phase is exhibited when PBT is cooled from the melt. Upon stretching, this is converted to the strained, or $\beta$-phase, which upon removal of the stress reverts back to the $\alpha$-phase. The major obvious distinctions between these two crystalline forms lies in the conformation of the tetramethylene segment and the crystallographic repeat dis-

* To whom correspondence should be addressed.

0024-9297/89/2222-1267$01.50/0 